Supplemental Material for Joint Token Pruning and Squeezing Towards More Aggressive Compression of Vision Transformers

Siyuan Wei[1*] Tianzhu Ye[2*] Shen Zhang[1] Yao Tang[1] Jiajun Liang[1†]
[1]MEGVII Technology [2]Tsinghua University
{weisiyuan, zhangshen,tangyao02,liangjiajun}@megvii.com,ytz20@mails.tsinghua.edu.cn

1. Overview

In the supplemental materials, we show the following details of our joint Token Pruning & Squeezing (TPS):

- Visualizations.
- Details of two variants.
- TPS on hybrid ViTs.
- Detailed experiment settings.
- TPS on larger models and with larger input size.
- TPS under different keep ratios.
- More ablations about TPS design.

2. Visualizations

We demonstrate the additional cases from ImageNet1K [1], which our TPS-DeiT and DeiT predict correctly but dynamicViT-DeiT predict wrongly. As Fig 2 shows, we found that the imperfect pruning policy brings the loss of background context and incomplete subject, which puzzles the model and leads to a close but incorrect prediction. However, our TPS conquers these cases by squeezing the information of pruned tokens into similar reserved tokens.

3. Details of Two Variants

We design two variants of TPS: dTPS and eTPS, to show our flexibility and compare fairly with dynamicViT [7] and EViT [5]. Theoretically, our TPS can be incorporated with any token pruning method. In this paper, we choose dynamicViT and EViT as baselines for their strong performance and concise forms. The major disparities between the two variants are as follows:

Forward procedure. The TPS module drops the tokens from inputs practically except for the training stage of dTPS. In each pruning stage, the dTPS module employs the gumbel-softmax [3] to sample binary decision mask randomly during training and maintain the presently reserved mask and pruned mask to avoid previously pruned tokens from participating in the matching and fusing step. In the subsequent attention layer, the attention masking strategy from dynamicViT [7] is employed to erase the effects of dropped tokens. The implementation details can be found in the code file.

Position to insert. As mentioned in the paper, dTPS and eTPS cut down tokens in inter-block and intra-block ways, respectively. The dTPS module is inserted before the transformer block, while the eTPS module is inserted after the multi-head attention layer. The distinction derives from the different token scoring methods. The learnable score prediction employed by dynamicViT and dTPS does not rely on any internal operation of transformer blocks, while the scoring based on the class-token attentions requires the results from the multi-head attention block.

Parameters. The eTPS module is parameter-free, while the dTPS module increases the total number of parameters by a small amount due to its learnable token score prediction head.

Performances. The performances of dTPS and eTPS modules are close but can be slightly different when training epochs changes. According to our experiments, the eTPS module outperforms the dTPS module under 30 epochs. The opposite results were observed under 100 epochs. The difference demonstrates that extra parameters of dTPS modules endow the model with a higher upper limit.

4. TPS on Hybrid ViTs

We conduct experiments on PVT [10] and CvT [11] to prove our design is compatible with hybrid ViTs.

4.1. PVT

Generally, We insert dTPS modules between the patch embedding layer and the subsequent basic block of each pruned stage. Unlike TPS on vanilla ViTs, we reserve atten-

*The first two authors contributed equally to this work
†Corresponding author

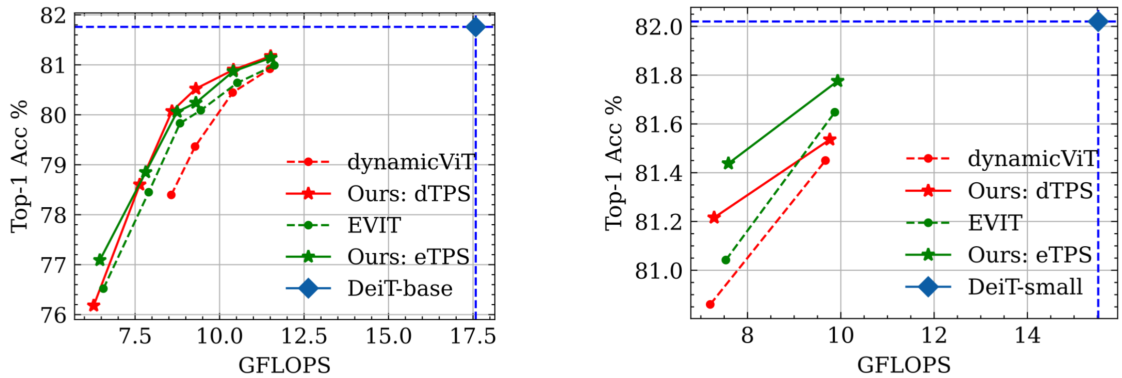

(a) Comparison on DeiT-B.

(b) Comparison on DeiT-S-384×384.

Figure 1. Note that dynamicViT can't converge in the two most aggressive pruning settings in (b).

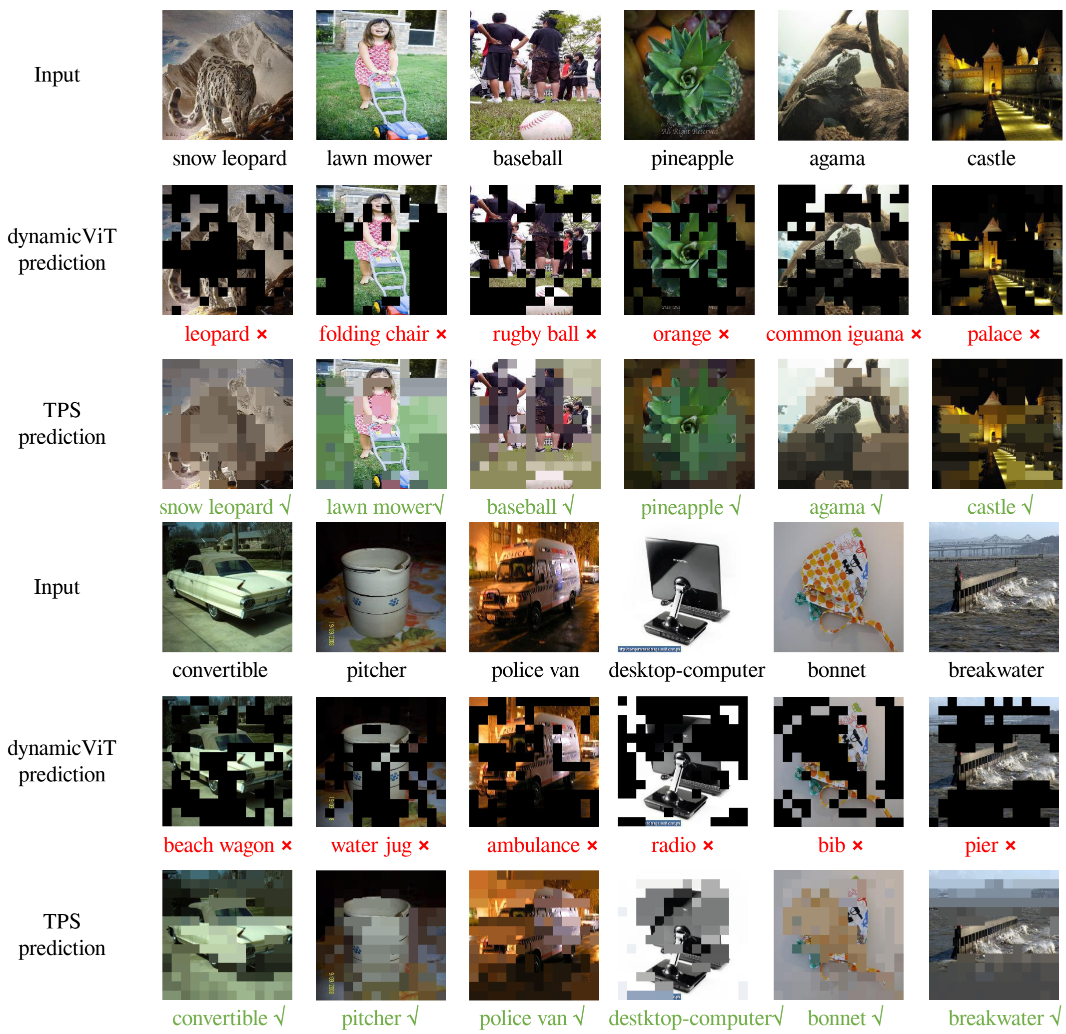

Figure 2. Comparisons between dynamicViT [7] and our joint Token Pruning & Squeezing. The results are given by dynamicViT-DeiT-small and our TPS-DeiT-small with the same pruning setup (pruning locations are $\{4^{th}, 7^{th}, 8^{th}\}$ and token keeping ratio of each pruning stage ρ is 0.5). The cases of dynamicViT and our TPS are displayed based on practical operations of the first stage with pruning applied. For dynamicViT, the blank tokens denote pruned ones; for our TPS, we mask each group of matched tokens in the TPS as the same color for visualization clarity.

Matching Method	Acc. (%)
N:1	**71.90**
1:1	69.02

(a) Different matching methods on dTPS-DeiT-T. The keep ratio is **0.7**.

Fusing Method	Policy	Acc. (%)
Weighting	Original	70.58
	Random	**65.56 (-5.02)**
Average	Original	70.47
	Random	65.173 (-5.30)

(b) Robustness comparison of fusing methods on dTPS-DeiT-T. The keep ratio is **0.5**.

Table 1. The pruned layers includes 4^{th},7^{th},8^{th}. (a) N:1 matching employed by TPS finds the nearest reserved token for each pruned token to inject multiple tokens into the same token, while 1:1 matching finds the nearest pruned token for each reserved token. (b) The similarity-weighting fusing obtains a lower accuracy drop under random token squeezing (see more details in the main paper: Sec. 4.3) than average fusing.

tive tokens from the whole tokens set in each pruned stage and utilize the masking or padding operations to maintain the complete spatial structure during training and inference, respectively.

Training. The spatial reduction layer of the basic block in PVT requires input with a complete spatial structure. For the basic block with a spatial reduction block, given the policy M, we maintain the complete spatial structure and mask the dropped tokens in key K and in value V with zeros before the spatial reduction layer as follows:

$$SRA^*(Q, K, V) = MHA(Q, SR(K \odot M), SR(V \odot M)) \quad (1)$$

Here, SRA^* is the modified spatial reduction attention, MHA is the multi-head attention operation, and SR is the spatial reduction layer. Moreover, we perform the same masking operation on dropped tokens before the patch embedding layer of next stage.

For the basic block without a spatial reduction layer, no masking operation is needed ,and we conduct the attention masking strategy from dynamicViT [7] to erase the effects of the dropped tokens.

Inference. The inference procedure of dTPS is adjusted slightly to practically accelerate the spatial reduction layer. The input tokens are pruned by a top-k selection operation based on the scoring results. For the block with a spatial reduction layer, we pad the previously dropped tokens with zero in the SRA^* to maintain the complete spatial structure.

$$K' = Pad(K, M) \quad (2)$$

$$V' = Pad(V, M) \quad (3)$$

$$SRA^*(Q, K, V) = MHA(Q, SR(M'), SR(V')) \quad (4)$$

Also, the same padding operation is utilized before the patch embedding layer of the next stage. For the block without a spatial reduction layer, no padding operation is needed either. The requirement of complete spatial structure leads to less shrinkage of computations.

4.2. CvT

The last stage of CvT [11] contains most of its blocks; therefore we only modify the last stage with our dTPS. The operations remain the same for other stages as the original CvT [11].

Training. The convolutional projection operation in CvT requires the input with a complete spatial structure. Given the policy M, we mask the dropped tokens with zeros before the convolution projection:

$$Q, K, V = ConvolutionalProjection(X \odot M) \quad (5)$$

Inference. The input tokens are pruned by a top-k selection operation based on the scoring results. To maintain the complete spatial structure, we pad the previously dropped tokens with zeros in the convolutional projection layer.

$$X' = Pad(X, M) \quad (6)$$

$$Q, K, V = ConvolutionalProjection(X') \quad (7)$$

ATS [2] conducts experiments on CvT [11] as well. It takes a variant of CvT [11] as the pre-trained model without convolutional projection in stage 3. It only performs token pruning in stage 3 to avoid the extra operation to maintain the structured spatial input. Compared to ATS [2], our method utilizes masking and padding during training and inference to keep the spatial structure.

5. Detailed Experiment Settings

5.1. ImageNet-1K Classification

All experiments follow the same data augmentations used in DeiT[1] [8]. All the model is initialized with pre-trained models' weights and fine-tuned with different token pruning location and token keeping ratio. We adopt the AdamW [6] as the optimizer and a cosine learning rate scheduler.

TPS on DeiT [8]. The experiment settings of dTPS-DeiT follows dynamicViT[2] except for basic learning rate

[1] https://github.com/facebookresearch/DeiT
[2] https://github.com/raoyongming/DynamicViT

is set to $\frac{batchsize}{1024} \times 2.5 \times 10^{-4}$ and no stage of fixing backbone weights. The experiment settings of eTPS-DeiT follow EViT[3]. The pruning settings include combinations of three multi-layer pruning settings: $prune\_locs \in \{[4,7,10],[3,5,7,9],[4,6,8,10]\}$, and two token keeping ratios :$\rho \in \{0.5, 0.7\}$. The token keeping ratio remains the same in all pruning stages.

TPS on LV-ViT [4]. The experiments of dTPS and eTPS on LV-ViT [4] follow the same training settings of dTPS and eTPS on DeiT, except for the basic learning rate is set to $\frac{batchsize}{1024} \times 1.0 \times 10^{-4}$ for the stable convergence. For LV-ViT-T, the pruning settings include combinations of three multi-layer pruning settings: $prune\_locs \in \{[4,7,10],[3,5,7,9],[4,6,8,10]\}$, and two token keeping ratios :$\rho \in \{0.5, 0.7\}$. For LV-ViT-S, the pruning settings include combinations of three multi-layer pruning settings: $prune\_locs \in \{[5,9,13],[3,6,9,12],[4,7,10,13]\}$, and two token keeping ratios :$\rho \in \{0.5, 0.7\}$.

TPS on PS-ViT [12]. The experiments of dTPS on PS-ViT [12] follow the same training settings as ATS [2] on PS-ViT [12]. The basic learning rate is set to $\frac{batchsize}{768} \times 5.0 \times 10^{-4}$, $prune\_locs$ is set to [3,6,9] and token keeping ratio ρ is 0.5.

TPS on PVT [10]. The pruning stages include stage 2, stage 3, and stage 4. The token keeping ratio for all dTPS modules is set to 0.7. Basic learning rate is set to $\frac{batchsize}{1024} \times 2.5 \times 10^{-4}$.

TPS on CvT [11]. The basic learning rate is set to $\frac{batchsize}{1024} \times 5.0 \times 10^{-5}$. The dTPS modules are only inserted into stage 3, and the pruning locations include [3,6,9] for CvT-13,[5,9,13] for CvT-21. The token keeping ratio for all TPS modules is set to 0.5.

5.2. iNaturalist 2019 Classification

TPS on DeiT [8]. For the experiment on iNaturalist 2019 Classification [9], we re-train DeiT and fine-tune the model with dynamicViT or dTPS applied.

In the training step, we initialize DeiT [8] with weights of ImageNet1K pre-trained model and re-train them for 300 epochs. The basic learning rate is set to $\frac{batchsize}{1024} \times 10^{-3}$. The other settings follow DeiT [8].

In the fine-tuning step, we initialize dynamicViT-DeiT and dTPS-DeiT with weights from the last step and fine-tune them for 30 epochs with the same pruning setup. The token pruning location is set to [4,7,10], and the token keeping ratio is 0.5. We follow the same fine-tuning settings as the experiments on ImageNet1K, except for no distillation loss.

[3] https://github.com/youweiliang/evit

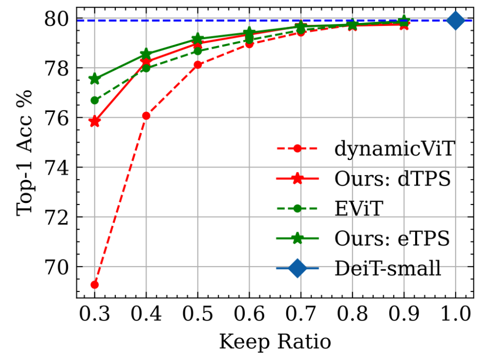

Figure 3. TPS under different keep ratios on DeiT-S.

6. TPS on Larger Models and with Larger Input Size

We conduct experiments of TPS on DeiT-B as shown in Fig. 1a to demonstrate it is compatible with large models. We also prove TPS can perform well with larger input size such as 384×384, as shown in Fig. 1b.

7. TPS under Different Keep Ratios

Experiments of TPS under different keep ratios are shown in Fig. 3.

8. More Ablations About TPS Design

More matching & fusing methods are shown in Tab. 1 as ablations about our TPS design. Tab. 1a indicates that TPS performance improvement benefits from compressing pruned tokens' information while unmatched reserved tokens remain unchanged. Token scoring can be proved necessary for squeezing under random token division meets a significant drop as shown in Tab. 1b and robustness analysis in the main paper: Sec. 4.3.

References

[1] Jia Deng, Wei Dong, Richard Socher, Li-Jia Li, Kai Li, and Li Fei-Fei. Imagenet: A large-scale hierarchical image database. In *2009 IEEE conference on computer vision and pattern recognition*, pages 248–255. Ieee, 2009. 1

[2] Mohsen Fayyaz, Soroush Abbasi Koohpayegani, Farnoush Rezaei, and Sommerlade1 Hamed Pirsiavash2 Juergen Gall. Adaptive token sampling for efficient vision transformers. 3, 4

[3] Eric Jang, Shixiang Gu, and Ben Poole. Categorical reparameterization with gumbel-softmax. *arXiv preprint arXiv:1611.01144*, 2016. 1

[4] Zi-Hang Jiang, Qibin Hou, Li Yuan, Daquan Zhou, Yujun Shi, Xiaojie Jin, Anran Wang, and Jiashi Feng. All tokens matter: Token labeling for training better vision transformers. *Advances in Neural Information Processing Systems*, 34:18590–18602, 2021. 4

[5] Youwei Liang, Chongjian Ge, Zhan Tong, Yibing Song, Jue Wang, and Pengtao Xie. Not all patches are what you need: Expediting vision transformers via token reorganizations. *arXiv preprint arXiv:2202.07800*, 2022. 1

[6] Ilya Loshchilov and Frank Hutter. Decoupled weight decay regularization. *arXiv preprint arXiv:1711.05101*, 2017. 3

[7] Yongming Rao, Wenliang Zhao, Benlin Liu, Jiwen Lu, Jie Zhou, and Cho-Jui Hsieh. Dynamicvit: Efficient vision transformers with dynamic token sparsification. *Advances in neural information processing systems*, 34:13937–13949, 2021. 1, 2, 3

[8] Hugo Touvron, Matthieu Cord, Matthijs Douze, Francisco Massa, Alexandre Sablayrolles, and Hervé Jégou. Training data-efficient image transformers & distillation through attention. In *International Conference on Machine Learning*, pages 10347–10357. PMLR, 2021. 3, 4

[9] Grant Van Horn, Oisin Mac Aodha, Yang Song, Yin Cui, Chen Sun, Alex Shepard, Hartwig Adam, Pietro Perona, and Serge Belongie. The inaturalist challenge 2019 dataset. *arXiv preprint arXiv:1707.06642*, 2019. 4

[10] Wenhai Wang, Enze Xie, Xiang Li, Deng-Ping Fan, Kaitao Song, Ding Liang, Tong Lu, Ping Luo, and Ling Shao. Pyramid vision transformer: A versatile backbone for dense prediction without convolutions. In *Proceedings of the IEEE/CVF International Conference on Computer Vision*, pages 568–578, 2021. 1, 4

[11] Haiping Wu, Bin Xiao, Noel Codella, Mengchen Liu, Xiyang Dai, Lu Yuan, and Lei Zhang. Cvt: Introducing convolutions to vision transformers. In *Proceedings of the IEEE/CVF International Conference on Computer Vision*, pages 22–31, 2021. 1, 3, 4

[12] Xiaoyu Yue, Shuyang Sun, Zhanghui Kuang, Meng Wei, Philip HS Torr, Wayne Zhang, and Dahua Lin. Vision transformer with progressive sampling. In *Proceedings of the IEEE/CVF International Conference on Computer Vision*, pages 387–396, 2021. 4